SUPPORTING INFORMATION FOR

Coupled Stream-Subsurface Exchange of Colloidal Hematite and Dissolved Zinc, Copper and Phosphate

Jianhong Ren* and Aaron I. Packman

Northwestern University, Department of Civil and Environmental Engineering, 2145 Sheridan Road, Evanston, Illinois 60208-3109, USA.

* Corresponding author. Now at Department of Environmental and Civil Engineering, MSC 213, Texas A&M University – Kingsville, Kingsville, Texas, 78363-8202, USA. Email: jianhong.ren@tamuk.edu, phone: 361-593-2798, fax: 361-593-2069.

The Number of Pages: 7 including cover sheet

The Number of Figures: 8

The Number of Tables: 2

Supplement 1: Hematite size distributions measured under different background water conditions by ZetaPALS and by settling column.

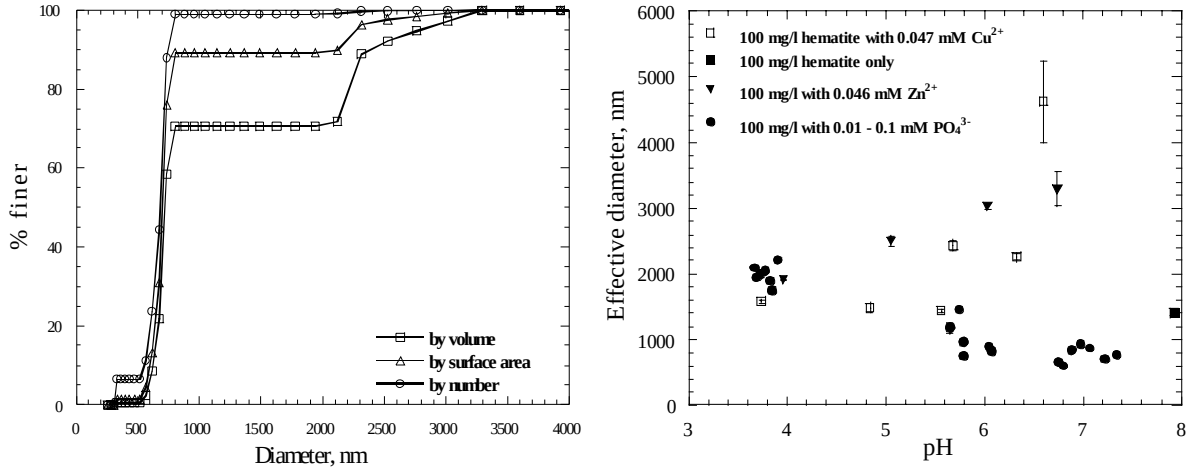

Figure S1. A) Size distribution of hematite used in run #1 under near-neutral conditions in weak NaCl background solution measured by ZetaPALS; B) Effective mean hematite size in the presence of Zn^{2+}, Cu^{2+}, and PO_4^{3-} measured by ZetaPALS. Error bars are ± 1 standard deviation based on three measurements.

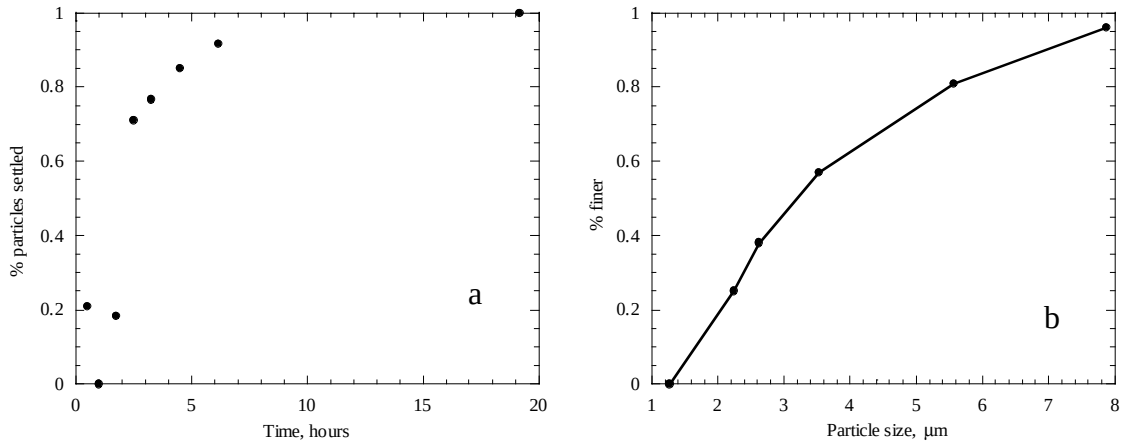

Figure S2. a) Hematite (used in runs #2-#6) deposition observed in a settling column with 3 mM NaCl at neural pH; b) Resulting particle size distribution.

Supplement 2: Experimental results and model fits used to estimate surface site densities and equilibrium constants for zinc, copper, and phosphate sorption to hematite and sand.

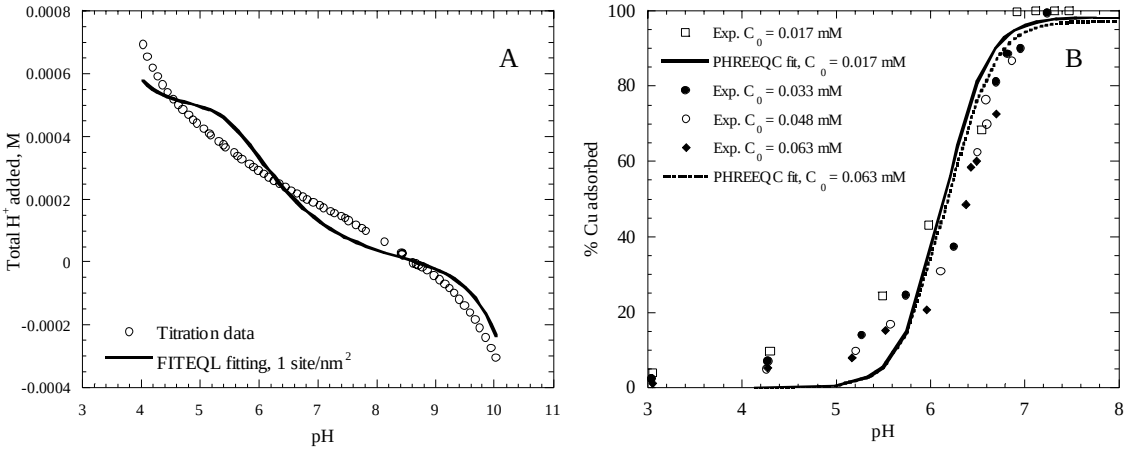

Figure S3. A) Surface titration of hematite with FITEQL fit; B) Representative batch sorption experiment results showing Cu sorption to hematite with PHREEQC fit.

Table S1: Surface site densities and equilibrium constants estimated by applying FITEQL to titration data and PHREEQC to batch sorption data.

Particles and Solutes	Surface site density, site/nm^2	LOGK_{a1}	LOGK_{a2}	LOGK_{eq}
Sand and Zn	27.90	0.39	-11.52	0.75
Sand and Cu	26.43	7.47	-9.45	2.38
Sand and PO_4^{3-}	1.91	7.47	-9.45	31.29, 25.39, 17.72
Hematite and Zn	6.65	25.07	7.39	17.50
Hematite and Cu	25.00	25.07	7.39	18.50
Hematite and PO_4^{3-}	1.50	4.42	6.17	32.29, 1.39, 34.92

Supplement 3: Filtration coefficients for hematite obtained from column experiments

Table S2. Measured filtration coefficients for hematite deposition in Ottawa #12 Flint silica sand under different background chemical conditions.

Background solutes	λ_f, cm^{-1}	pH
10 mM NaCl	0.56	6.94
10 mM NaCl and 0.01 mM PO_4^{3-}	0.0097	7.42
10 mM NaCl and 0.01 mM PO_4^{3-}	0.03	6.77
10 mM NaCl and 0.10 mM PO_4^{3-}	0.0078	6.71
10 mM NaCl and 0.02 mM Zn^{2+}	1.76	7.07

Supplement 4: Results of individual experiments on colloid and solute exchange with a sand bed in a recirculating flume.

The in-stream concentration data and model predictions for flume experiment #1 with Zn are compared in Figure S4. A dimensionless colloid settling velocity of $v_s^* = 0.42$ was calculated from the measured particle size of 3.3 μm. This dimensionless settling velocity was used to predict the exchange of both hematite and Zn in run 1, and the results are shown in Figure S4a. The exchange of hematite was predicted reasonably well using an effective diameter of 3.3 μm, but both total and dissolved zinc exchange were over-predicted. When an input dimensionless settling velocity of $v_s^* = 0.1$ was used, corresponding to a particle diameter of 1.5 μm, the model predictions of both total and dissolved Zn exchange improved significantly as shown in Figure S4b. However, use of $v_s^* = 0.1$ significantly under-predicted the observed hematite exchange.

These seemingly irreconcilable results are explained by the fact that the hematite size distribution was actually bimodal, as shown in Figure S1 (Supplement 1). The bulk of the hematite surface area occurs on particles with a diameter of 700 – 800 nm, but the size distribution by volume shows a significant fraction at 2.3 μm. These observations, combined with the flume data, indicate that Zn transport occurred predominantly on the smaller hematite size class while bulk hematite deposition was controlled by the mean particle size. Thus, the particles carrying the bulk of the colloidal-phase Zn deposited at a rate substantially less than the mean hematite deposition rate.

The comparisons of model predictions with the results of Runs #2-#4 with Zn and Cu are shown in Figures S5 and S6, respectively. The removal of total Zn, Cu, and hematite from the surface water was predicted reasonably well in these experiments using the new multi-phase contaminant transport model. The hematite used in these three experiments was prepared separately from the hematite used in Run #1, and was not bimodal, so one effective diameter could be used to simultaneously predict both hematite and metal exchange. Discrepancies between model predictions and flume results for copper at later times in Runs #3 and #4 are attributed to the precipitation of a colloidal copper phase. Independent batch experiments showed that Cu starts to form a precipitate under the flume experimental conditions as a pH of around 6.5, with additional precipitation occurring at higher pH. As shown in Figure S7, the stream pH was initially lower than 6.6 in runs #3 and #4, but it increased over time. In Run #3, the pH became greater than 6.6 after 20 hours ($t^* = 150$), while in run #4 the pH increased to around 6.5 after 13 hours ($t^* = 84$) and then stabilized between 6.5 and 6.6. The slightly higher pH induced copper precipitation, which caused additional copper to deposit in the streambed. The higher pH in Run #3 caused greater copper precipitation, and thus a greater discrepancy between the model prediction and the flume data.

The comparisons of model predictions and flume experiment results of Runs #5 and #6 with phosphate are shown in Figure S8. The model predictions for Run #5 agree well with the flume data, but the model substantially under-predicts phosphate exchange in Run #6. The phosphate concentration was 11 mg/l (0.12 mM) in Run #6. Batch sorption experiments showed that the adsorption of phosphate to sand was nonlinear at such a high phosphate concentration, but the nonlinear sorption process could not be included in the multi-phase exchange model because of computational constraints.

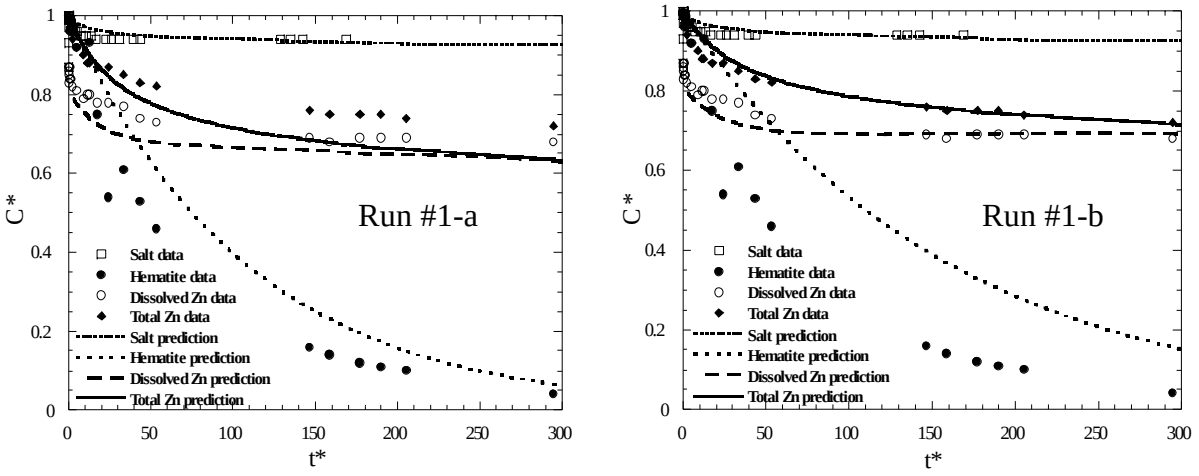

Figure S4. Comparison of experimental results and model predictions for Run #1 with Zn^{2+}. Modeled hematite diameters: a) d_p = 3.3 μm; b) d_p = 1.5 μm.

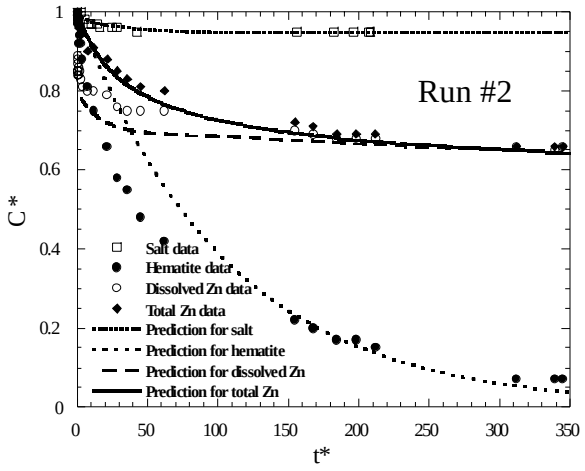

Figure S5. Comparison of experimental results and model predictions for Run #2 with Zn^{2+}.

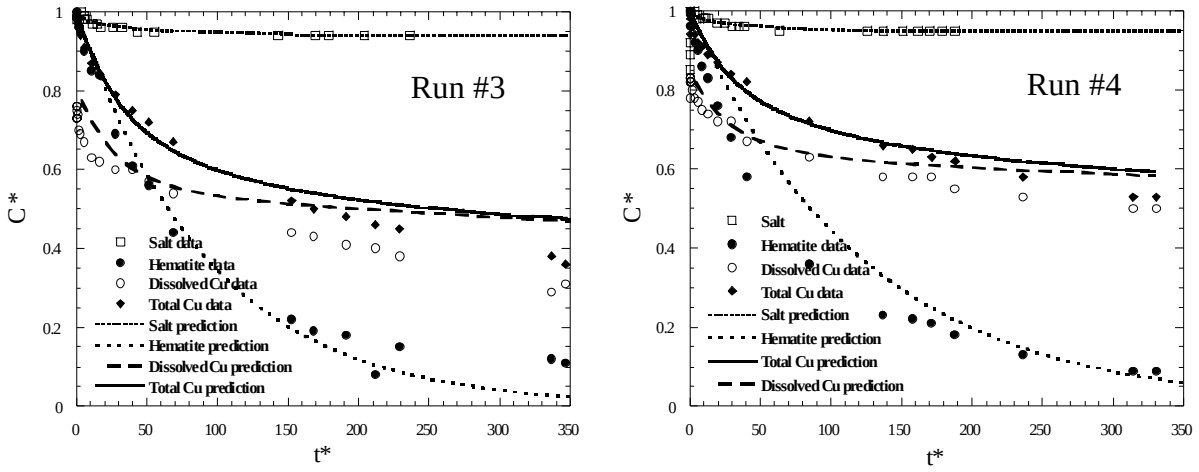

Figure S6. Comparisons of exchange data and model predictions for Runs #3- #4 with Cu^{2+}.

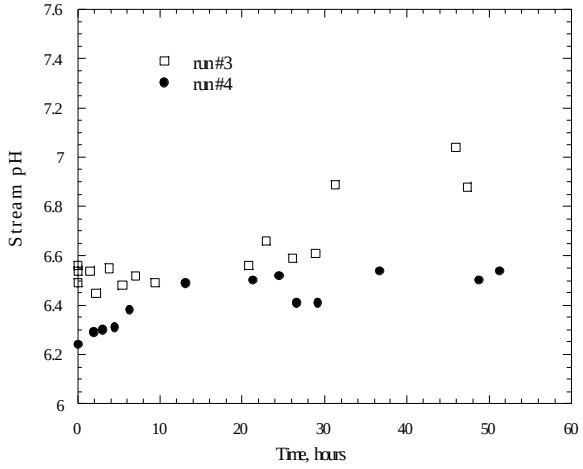

Figure S7. Changing stream pH observed in Runs #3 and #4 with Cu^{2+}.

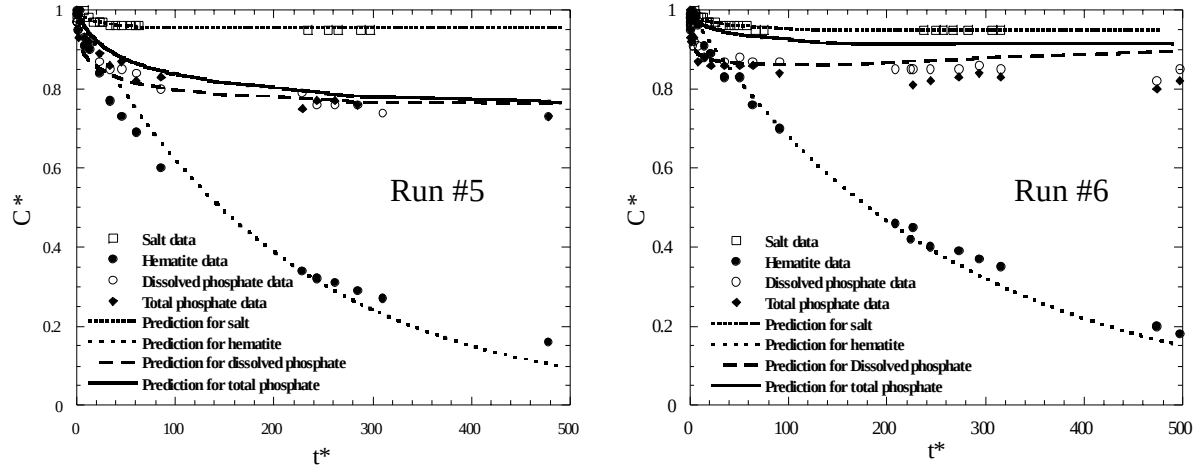

Figure S8. Comparisons of exchange data and model predictions for Runs #5 and #6 with phosphate.